remote sensing

MDPI

Article

Radiometric Performance of the TerraSAR-X Mission over More Than Ten Years of Operation

Marco Schwerdt *, Kersten Schmidt, Patrick Klenk, Núria Tous Ramon, Daniel Rudolf, Sebastian Raab, Klaus Weidenhaupt, Jens Reimann and Manfred Zink

German Aerospace Center (DLR), Microwaves and Radar Institute, Oberpfaffenhofen, D-82234 Wessling, Germany; kersten.schmidt@dlr.de (K.S.); patrick.klenk@dlr.de (P.K.); nuria.tousramon@dlr.de (N.T.R.); daniel.rudolf@dlr.de (D.R.); sebastian.raab@dlr.de (S.R.); klaus.weidenhaupt@dlr.de (K.W.); jens.reimann@dlr.de (J.R.); manfred.zink@dlr.de (M.Z.)

* Correspondence: marco.schwerdt@dlr.de; Tel.: +49-8153-28-3533

Received: 23 April 2018; Accepted: 13 May 2018; Published: 15 May 2018

Abstract: The TerraSAR-X mission, based on two satellites, has produced SAR data products of high quality for a number of scientific and commercial applications for more than ten years. To guarantee the stability and the reliability of these highly accurate SAR data products, both systems were first accurately calibrated during their respective commissioning phases and have been permanently monitored since then. Based on a short description of the methods applied, this paper focuses on the radiometric performance including the gain and phase properties of the transmit/receiver modules, the antenna pattern checked by evaluating scenes acquired over uniformly distributed targets and the radiometric stability derived from permanently deployed point targets. The outcome demonstrates the remarkable performance of both systems since their respective launch.

Keywords: TerraSAR-X; internal calibration; geometric and radiometric calibration; antenna model verification; antenna pointing determination; radiometric accuracy; calibration targets; long term performance monitoring

---

1. Introduction

More than ten years ago, on 15 June 2007, the first German synthetic aperture radar (SAR) mission TerraSAR-X for commercial and scientific application was started by launching the first satellite, called TSX. Three years later, in June 2010, the mission was expanded by an additional satellite, TDX. Since then, both satellites have been flying in a close formation in a sun-synchronous dusk-dawn orbit at 514 km altitude to fulfill the tasks of two different missions in parallel:

- the TerraSAR-X mission for providing single multi-mode X- Band SAR data in different operation modes [1] and
- in bistatic operation, the TanDEM-X mission to generate a new global digital elevation model on a 12-m grid and a vertical accuracy better than two meters [2].

The satellites feature an advanced high-resolution X-Band SAR instrument operated at 9.65 GHz and enabling the operation in Spotlight, Stripmap and ScanSAR mode, in different polarizations and over a wide range of incidence angles. For these various acquisition modes, their active phased array antenna electronically steers and shapes the patterns in the azimuth and elevation direction. The antenna consists of 12 panels in azimuth direction with each panel comprising 32 sub-array radiators in elevation direction, whereby each sub-array is fed by its own active transmit/receiver module (TRM). The instrument combines the ability to acquire high resolution images for detailed analysis as well as wide swath images for overview applications. The geometric resolution varies from

0.24 m for Staring Spotlight [3], 1 m for Spotlight, 3 m for nominal Stripmap, 16 m for ScanSAR and 40 m for Wide ScanSAR products. The image width ranges from 4.6 km (Staring Spotlight) to 266 km (Wide ScanSAR). There are over 1000 possible product variations, which result from the combination of different imaging modes, polarizations and elevation angles [4].

This paper focuses on the radiometric performance of the two satellites. A pre-requisite to ensure accurate and reliable SAR data products over the whole mission time is first, an accurate calibration of the system and, then, a permanent monitoring of relevant system parameters. During their commissioning phases, TSX (in 2007) and TDX (in 2010) could be accurately calibrated with outstanding results [5,6]. Since then, both SAR systems have been permanently monitored to detect changes in their performance, like degradation of the satellite hardware and to guarantee reliable and correct operation of the instruments. However, during a second TSX calibration campaign executed for the so called Dual Receive Antenna mode in 2009, a high radiometric stability could be verified two years after launch [7].

The evaluation of long-term system monitoring (LTSM) parameters, like instrument characteristics or the antenna patterns, verify an excellent stability of TSX and TDX. This LTSM has been ensuring a consistent product quality for more than ten years. The success of this performance is based on the innovative design and precise manufacturing of the satellite systems [8,9] on the one hand and on the other on innovative methods, accurate reference targets and the strategy for calibrating and monitoring TSX and TDX over lifetime [5,10–15]. The radiometric performance over lifetime of both systems is analyzed in three steps:

- characterizing the gain and phase stability of TRMs (Section 2) by means of coded calibration pulses,
- monitoring the antenna characteristics by evaluating scenes acquired over distributed targets like the Amazon rain forest (Section 3) and
- analyzing the radiometric stability by means of impulse response functions derived from permanently installed corner reflectors (Section 4).

Beyond that, the quality of SAR data products have also been monitored since launch (Section 5).

2. Stability of Individual Transmit/Receiver Modules

For analyzing the stability of the TRMs within the instrument front end, the pseudo noise (PN) gating method is applied [16]. This method was developed and established in the frame of TerraSAR-X for characterizing the amplitude and phase settings of individual TRMs of an active phased array antenna, while all modules are in operation. Thus, all modules are characterized simultaneously under most realistic conditions—in contrast to switch on/off individual modules resulting in different power loads and consequently to nonrealistic operating conditions. Under the control of the Data and Control Electronics, the phase of each TRM is individually shifted between successive calibration pulses according to a certain code sequence. Based on these specific PN-gating data takes (L0 products), the settings of all TRMs are regularly monitored on transmission and on reception in flight.

Possible drift effects can be found by depicting amplitude and phase trends over time. For example, amplitude and phase deviations with respect to a reference value are plotted in Figure 1 for TSX versus data take execution time for each of the 384 TRMs on transmission. The reference value for each TRM was derived in flight at the beginning of the commissioning phase. The figure shows that all TRMs have been working within the established limits (red lines) so far, and only one outlier was detected in October 2012. To further monitor the TRMs status in detail at that time, several extra PN-gating data takes were ordered, but no further anomalies could be observed, as shown in Figure 1. Hence, no trend can be observed, indicating the stability of the TSX instrument and the TRM settings, respectively.

This characterization of individual TRMs has been performed for TSX and TDX over mission time since launch in 2007 and 2010, respectively. The results, averaged for each TRM over mission elapsed time, are shown in Figure 2 for the measured amplitude settings and in Figure 3 for the phase settings; red lines and black error bars indicate the mean value and standard deviation for each module, respectively.

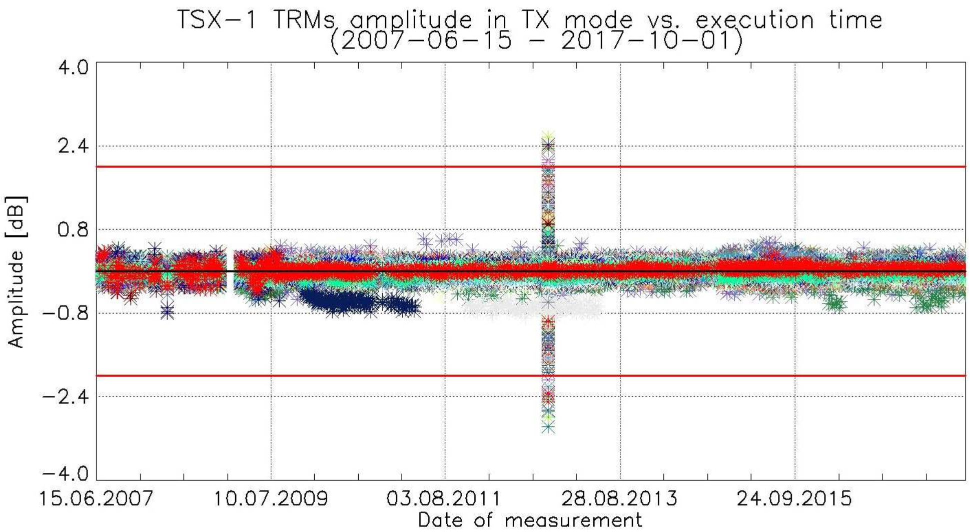

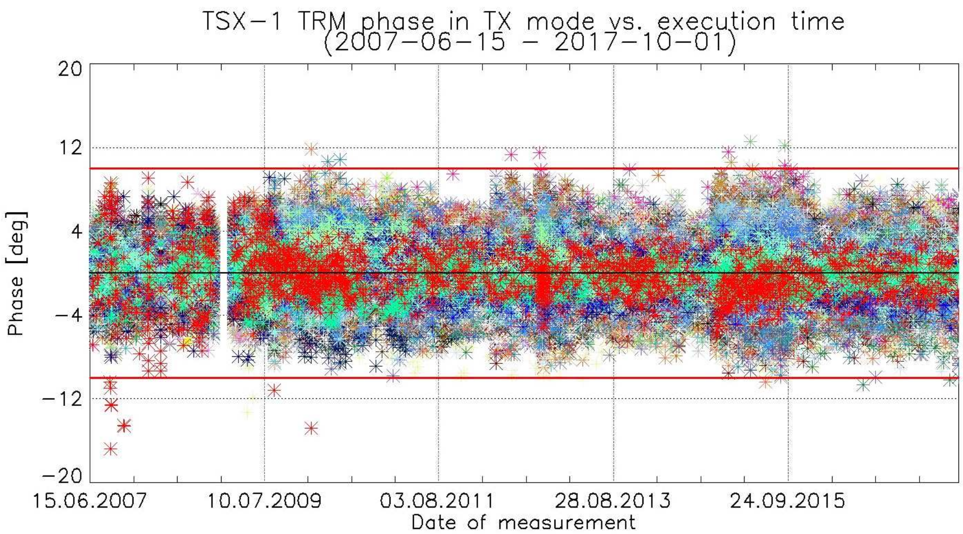

Figure 1. Amplitude and phase deviation versus time of all 384 transmit/receiver modules of TSX measured in flight since launch. Each colored dot along the y-axis indicates the measured deviation of one of the 384 TRMs at that time. Red horizontal lines indicate the established limits.

The figures show that the TRM amplitude and phase settings are very stable for transmission and reception: no instrument degradation is detectable for both satellites. Averaging the standard deviations over all modules yields an overview of the instrument quality for each parameter. The results are summarized in Table 1. The amplitude deviation stays below 0.2 dB, the phase deviation below 2.0 °. This is in the order of the accuracy of the PN gating method. It can be summarized that the TRMs have been working in a very stable manner over mission elapsed time, i.e., for more than 10 years for TSX and seven years for TDX.

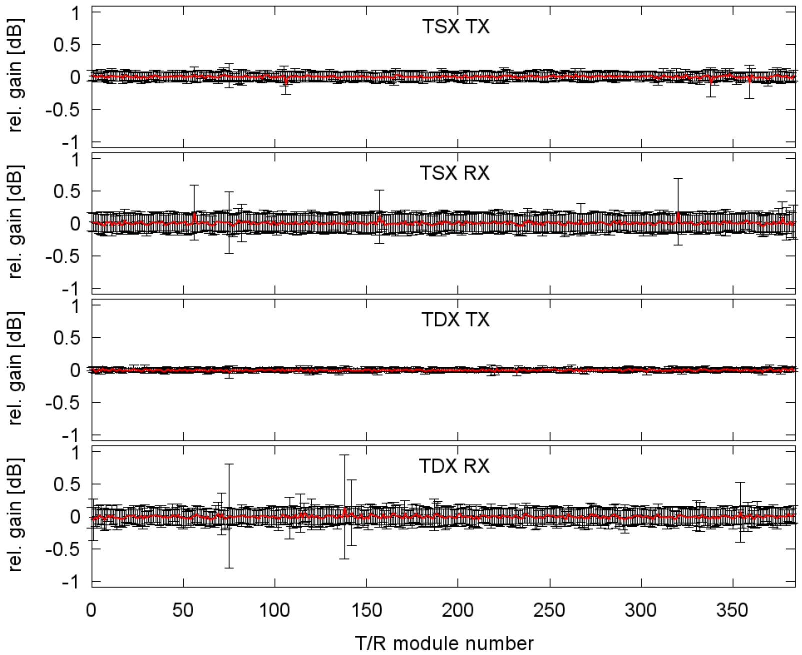

Figure 2. Amplitude deviation versus TRM number on transmission (TX) and reception (RX) for each of the 384 TRMs measured in flight since launch of TSX in 2007 (**top**) and TDX in 2010 (**bottom**). Red curve: the mean value averaged for each TRM over mission elapsed time, black error bars: corresponding standard deviation.

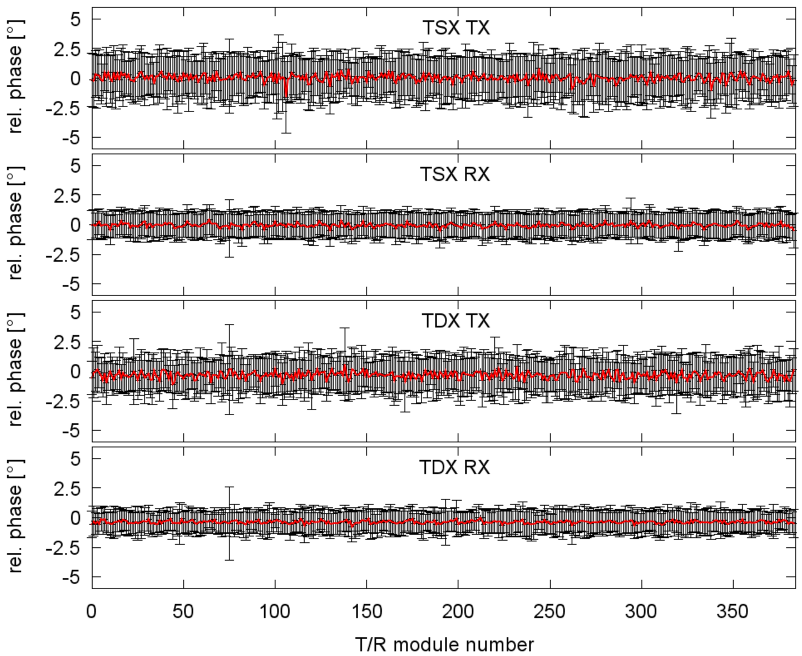

Figure 3. Phase deviation versus TRM number on transmission (TX) and reception (RX) for each of the 384 TRMs measured in flight since launch of TSX in 2007 (**top**) and TDX in 2010 (**bottom**). Red curve: the mean value averaged for each TRM over mission elapsed time, black error bars: corresponding standard deviation.

Table 1. Statistics of amplitude and phase TRM deviations on transmission and reception for TSX and TDX since launch.

Mean of the σ-values of all TRMs	TX		RX	
	Amplitude (dB)	**Phase** (°)	**Amplitude** (dB)	**Phase** (°)
TSX	0.08	1.97	0.16	1.16
TDX	0.03	1.67	0.14	1.05

3. Antenna-Pattern Monitoring

Besides internal calibration, the antenna patterns also have to be monitored to detect any degradation of the front-end panels; this concerns especially potential degradations of the antenna wave guides as these are not covered by internal calibration. For estimating the front-end quality, gamma profiles derived from SAR images acquired over the Amazon rainforest (Figure 4) are compared with antenna reference patterns calculated by means of a precise antenna model [17].

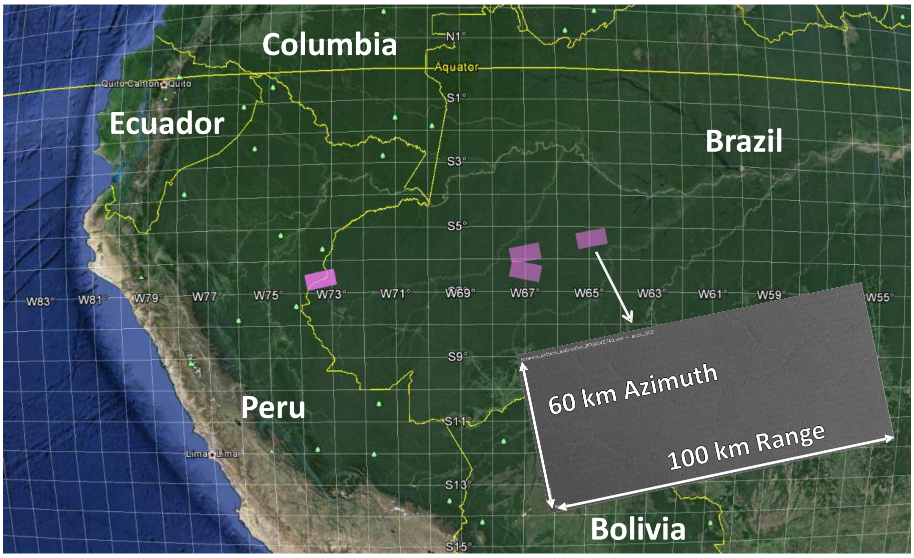

Figure 4. Four acquisition areas (pink) for long term system monitoring of the antenna over the Amazon rainforest serving as quite homogeneous scatterer as seen in the SAR image preview.

According to the strategy described in [5], the instrument is operated in ScanSAR mode for this monitoring task. For ScanSAR acquisitions, the beam is switched sequentially from burst to burst between four neighbouring subswaths to get a broader swath width compared to normal Stripmap acquisitions. By generating an un-normalized gamma profile for each of the four subswaths, the relative gain deviation from subswath to subswath can be determined (in Level1B products, the four subswaths are still separated but combined in a higher level product). Thus, not only the pattern shape of each single beam itself, but also the gain offset between different beams can be verified in flight. For this in-flight verification of the shape and the gain offsets, a strong requirement of ±0.2 dB was defined for the antenna model. The reason for that number was not only driven by the radiometric accuracy budget, but also by the visibility of gain offsets between adjoining beams in ScanSAR images.

An essential assumption for the analysis is a nearly constant gamma profile from rainforest backscattering. This was analyzed for different areas and acquisition periods by TSX and TDX in [18]. In this analysis, higher gamma values were measured for morning acquisitions (descending orbit) compared to afternoon acquisitions (ascending orbit). Hence, an absolute gain comparison over time is infeasible. Nevertheless, the rainforest can still be used to estimate the relative radiometric accuracy and the radiometric stability of the antenna pattern as each ScanSAR acquisition is evaluated separately. A typical measured uncorrected profile together with the antenna reference pattern is depicted on the top panel of Figure 5 for a single ScanSAR acquisition. Note that absolute radiometric calibration was performed by measuring both systems against accurate reference targets [5–7,11].

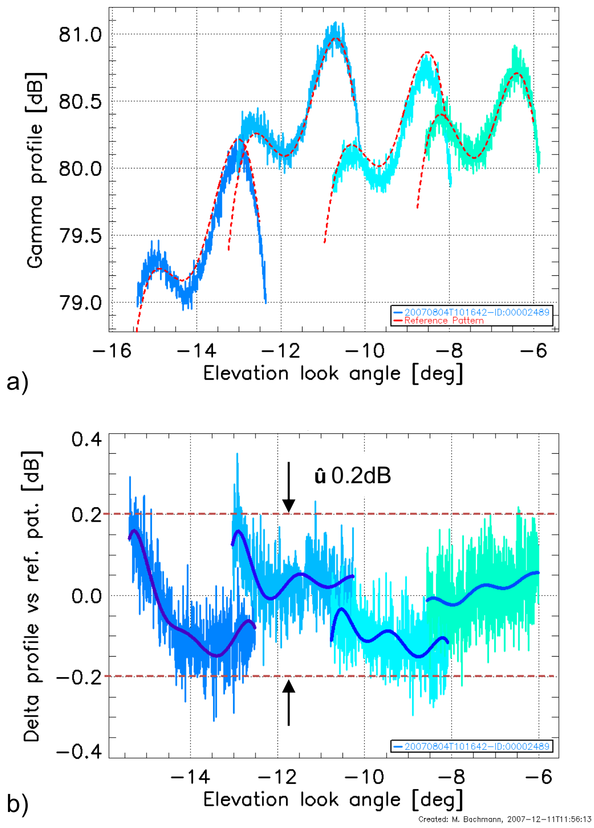

Figure 5. (**a**) antenna reference pattern (dashed red) and gain profiles (blue to green) derived from a ScanSAR image without pattern correction. (**b**) difference between reference and measured pattern to verify the antenna model w.r.t. pattern shape and beam-to-beam gain offset (blue lines are fits of the difference).

In the next step, the minimum and the maximum value as well as the standard deviation are derived from the difference between the reference and the measured antenna patterns, as shown on the bottom panel of Figure 5. Based on these statistic values derived from each set of ScanSAR beams acquired over the Amazon rainforest, the antenna patterns and consequently the front-end panels, especially the antenna wave guides have been monitored since launch of the satellites. This is shown in Figure 6: blue for TSX and green for TDX. Here, the minimum and maximum deviation between the measured and the calculated set of Scan-SAR patterns (four beams) per acquisition are represented by an error bar and the standard deviation by a triangle. Furthermore, the mean values are subtracted to focus on relative radiometric accuracy.

The standard deviation observed from mid-2014 until mid-2017 is slightly higher than during other mission times. This can be traced back to including a larger number of data takes (but acquired over the same test sites shown in Figure 4) in the LTSM analysis during that period, which were affected by weather-related effects such as heavy thunderstorms across the Amazon rainforest. From summer 2017 onwards, a stricter screening policy was adopted again, reducing the observed standard deviation to pre-2014 levels. Nevertheless, the timeline shows a very stable behavior of the antenna pattern. While the standard deviations are almost always inside a limit of +/−0.2 dB (with very few execeptions), the extreme values do not exceed +/−0.3 dB (excluding data takes disturbed by poor weather conditions). Finally, there is no remarkable difference between TSX and TDX.

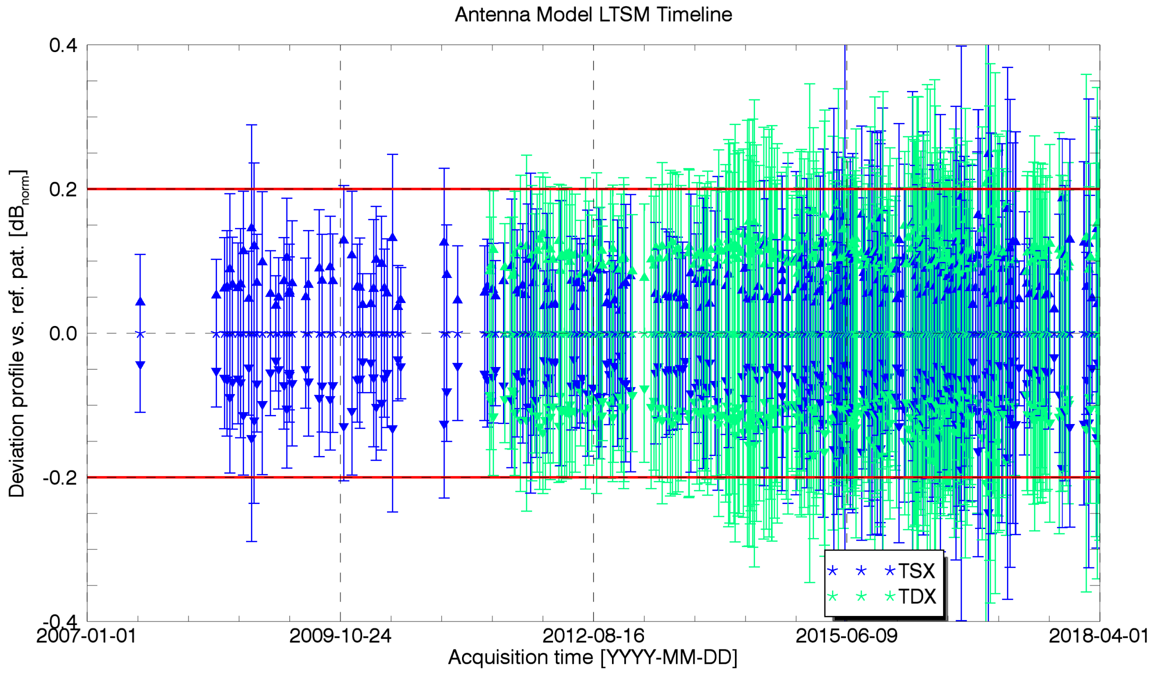

Figure 6. Timeline of antenna pattern statistics derived from SAR scenes acquired over the Amazon rainforest by using ScanSAR mode for TSX (blue) and TDX (green).

4. Radiometric Stability

The radiometric stability is monitored by deriving the radar cross section (RCS) of permanently installed corner reflectors. For this long-term system monitoring, three corner reflectors with a leg length of 1.5 m are permanently installed with fixed alignment near Neustrelitz, Germany (see Figure 7).

The RCS of each corner reflector has been monitored for more than 10 years for TSX and seven years for TDX. The results are shown in Figure 8. First of all, we can see that the theoretical RCS value of 43.42 dBm^2 in X-Band could be metrologically proven for all three corner reflectors by means of TSX and TDX. This confirms both how accurately the two systems were absolutely calibrated and matched to each other during their commissioning phases in 2007 [5] and 2010 [6] (by means of a mix of corner reflectors and transponders), and how accurately the corner reflectors were manufactured—because the mechanical tolerance of a corner reflector defines its absolute radiometric accuracy (1 mm form tolerance corresponds to about 0.2 dB accuracy).

Based upon a dedicated calibration campaign performed for TSX two years after the launch, a precise evaluation of the radiometric stability with a high confidence level could be achieved for TSX [7]. For this purpose, the absolute calibration factor derived from point target measurements executed in 2009 had been compared to that derived during the commissioning phase in 2007. The difference between both factors and consequently the radiometric stability over two years was only 0.15 dB. This stability was more than one magnitude better than the requirement of 0.5 dB over six months. However, a radiometric stability of 0.15 dB over two years would mean that the calibration factor might differ up to 0.75 dB from the initial value after ten years. However, this is not the case. As shown in Figure 8, the RCS values measured for each corner reflector are very stable, confirming as well a very stable radiometric performance of TSX and TDX for the entire duration of their mission time. The standard deviation over this period is below 0.2 dB and indicates that the calibration factor has not been drifting since launch. Hence, the high radiometric stability already explicitly derived in 2009 [7] remains valid over a much longer time period of 10 years.

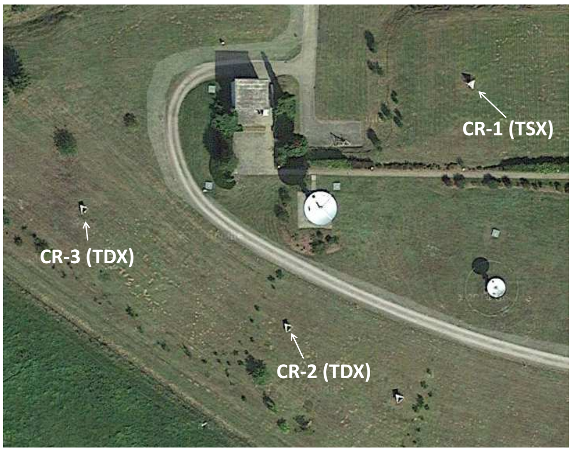

(**a**)

(**b**)

Figure 7. DLR calibration site for long-term system monitoring of TSX and TDX near Neustrelitz (Germany) with three permanently installed corner reflectors; (**a**) seen from the above; (**b**) closer view of one 1.5 m target showing the fixed alignment.

Moreover, as no trends and no degradation of the two systems can be observed, TSX and TDX still have the same absolute radiometric accuracy as the one derived by a comprehensive calibration campaign executed for both systems during the TDX commissioning phase in 2010 [6]. The radiometric performance of TSX and TDX are summarized in Table 2 and confirms that the satellites are still calibrated to unprecedented quality, 10 and seven years after launch of TSX and TDX, respectively.

Table 2. Radiometric performance parameters for TSX and TDX.

Cal Procedure	Goal	TSX	TDX
Internal Calibration			
Amplitude	0.25 dB	<0.1 dB	<0.1 dB
Phase	1.0 deg	<1.0 deg	<1.0 deg
TRM Setting Characterization			
Amplitude	-	<0.2 dB	<2 deg
Phase	-	<0.2 dB	<2 deg
Antenna Model Verification			
Pattern Shape	±0.2 dB	±0.2 dB	±0.2 dB
Beam-to-BeamGain Offset	±0.2 dB	±0.2 dB	±0.2 dB
Radiometric Calibration			
Radiometric Stability	0.5 dB *	<0.15 dB **	<0.15 dB **
Relative Accuracy	0.68 dB ‡	≤ 0.18 dB ‡	≤0.17 dB ‡
Absolute Accuracy	1.1 dB ‡	<0.34 dB ‡	<0.33 dB ‡

* requirement defined over a period of six months, ** measured by TSX after two years and confirmed by long term system monotoring over 10 years, ‡ StripMap mode.

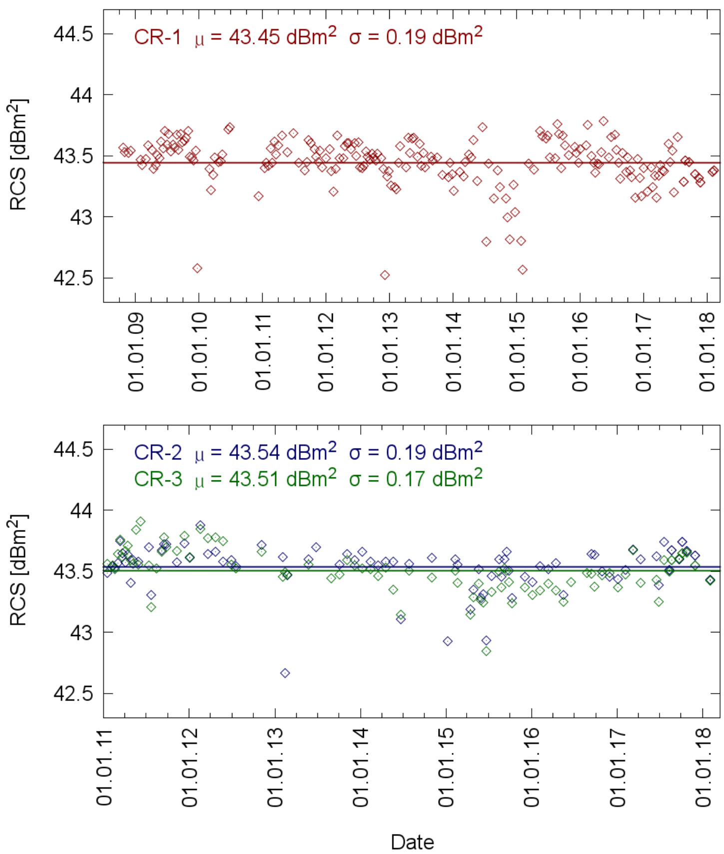

Figure 8. Radar cross section (RCS) of permanently installed corner reflectors derived from SAR images acquired by TSX (**top**) and TDX (**bottom**) over elapsed lifetime.

It should be mentioned that the absolute radiometric accuracy of <0.34 dB in Table 2 is composed of different independent error contributions: the error due to external calibration executed during the commissioning phase (0.16 dB for TSX and 0.14 dB for TDX), the stability of the instrument (<0.15 dB for TSX and TDX), a dynamic range error (0.1 dB for TSX and TDX) as well as an atmospheric loss error (0.24 dB to consider up to moderate rain fall in X-band [19]).

5. Image Quality

In addition to the radiometric performance of the instrument, the quality of SAR images also have been monitored for TSX and TDX since launch. Based on the impulse response function (IRF) derived from the three corner reflectors deployed within DLR's calibration site at Neustrelitz, the following parameters have been derived:

- integrated side lobe ratio (ISLR),
- peak-to-side lobe ratio (PSLR) and
- geometric resolution derived by the main lobe width at –3 dB.

The ISLR and PSLR are separated for azimuth and range direction and depicted in Figure 9 over the mission elapsed time. The statistics show a stable behavior for both satellites, the distributions are all inside the limit and essentially better than the required –18 dB for all parameters.

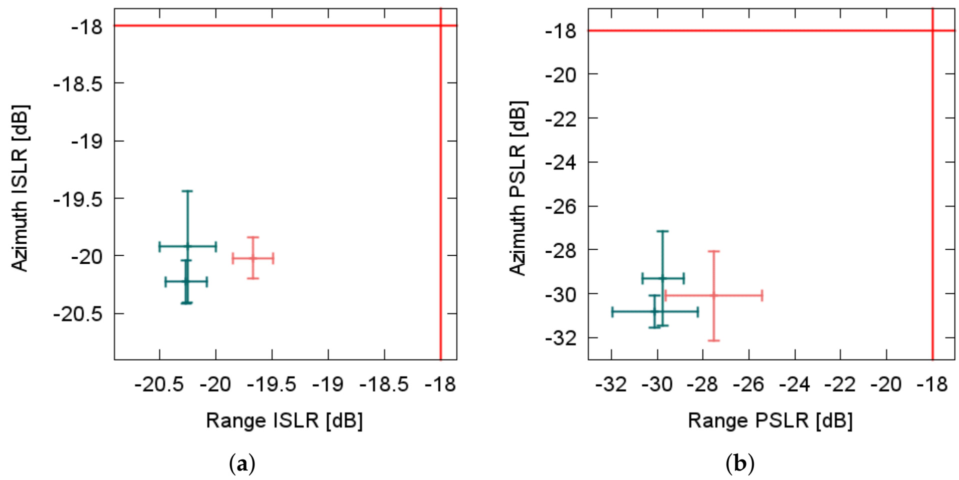

Figure 9. Statistics of image quality parameters derived from the IRF of permanently installed corner reflectors for TSX (red) and TDX (green); (**a**) intergated side lobe ratio (ISLR); (**b**) peak to side lobe ratio (PSLR). The center of the cross indicates the mean and the size of the cross the standard deviation in azimuth and range direction, respectively. All distributions are inside the limits (red lines).

The geometric resolution derived likewise from the corresponding IRF is shown in Figure 10 for TSX and TDX. The resolution of both systems is always inside the limit and essentially better than the required 1.8 m in range and 3.3 m in azimuth. The standard deviation for both systems is better than 1 cm in both direction and confirms likewise the constant product quality over mission time.

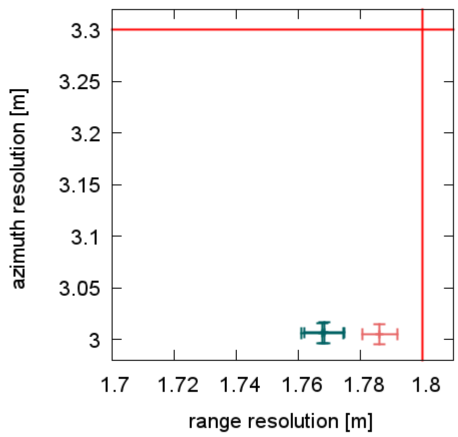

Figure 10. Geometric resolution in StripMap operation derived from the IRF of permanently installed corner reflectors for TSX (red) and TDX (green), the center of the cross indicates the mean and the size of the cross the standard deviation in azimuth and in range direction respectively. All distributions are inside the limits (red lines).

6. Conclusions

The radiometric performance of TSX and TDX has been monitored for the entire mission duration, i.e., more than 10 years for TSX and seven years for TDX. The measurements and extended analyses performed for this long-term system monitoring task show an outstanding stability of the instrument performance. No trends and no degradation have been observed and all parameters show a constant behavior since launch of the respective satellite. Moreover, the measurements against corner reflectors executed for TSX and TDX confirm first a high radiometric stability on the order of one tenth of a dB over a period of 10 years, which is considerably better than that one verified in flight by a dedicated calibration campaign executed in 2009, and second that the absolute radiometric accuracy derived by a comprehensive calibration campaign executed in 2010 is still valid for TSX and TDX.

Never before have two independent spaceborne SAR systems been as accurately calibrated and consequently matched to each other as TSX and TDX. All requirements and goals were not only achieved or succeeded during their individual commissioning phase. They are still valid, 10 and seven years after launch of TSX and TDX, respectively (see Table 2). This confirms not only that the performance of the satellites is still of unprecedented quality, but this also reflects the reliability and the accuracy of sophisticated procedures, modules and reference targets established for calibrating and monitoring both systems over lifetime. Thus, SAR data products of constant high quality have been provided for more than 10 years, and it is not distinguishable whether a TerraSAR-X scene was acquired by TSX or TDX. They are still perfect twins operated as SAR systems in space.

Author Contributions: M.S. had the leading role for preparing this article. By means of point target analysis, K.S. evaluated the radiometric stability and the quality of the SAR data. The work of P.K. was concentrated on the antenna and the verification of the antenna patterns. N.T.R. conducted the characterization of individual transmit/receive modules in the front end. D.R., S.R. and K.W. are responsible for the maintenance and the alignment of the reference targets. J.R. and M.Z. have contributed to the revision of this paper and provided insightful comments and suggestions. The manuscript was written by M.S. All authors have read and approved the final manuscript.

Acknowledgments: The authors would like to thank the whole TerraSAR-X team, particularly the calibration and operation teams of the Microwave and Radar Institute for intensively analyzing and commanding special calibration data takes and initiating automatic long-term system monitoring. But also great thank to Airbus Defence and Space GmbH for developing TerraSAR-X to be such a highly accurate and stable SAR system, a prerequisite for ensuring products of high quality over mission time. And finally the DLR colleagues of the Neustrelitz site for freeing the corner reflectors from snow during the winter.

Conflicts of Interest: The authors declare no conflict of interest.

Abbreviations

The following abbreviations are used in this manuscript:

DLR	German Aerospace Center
IRF	Impulse Response Function
ISLR	Integrated Side Lobe Ratio
LTSM	Long Term System Moniotring
PN	Pseudo Noise
PSLR	Peak to Side Lobe Ratio
RCS	Radar Cross Section
RX	Reception
SAR	Synthetic Aperture Radar
TDX	Second Satellite of the TerraSAR-X Mission
TRM	Transmit/Receiver Module
TSX	First Satellite of the TerraSAR-X Mission
TX	Transmission

References

1. Buckreuss, S.; Werninghaus, R.; Pitz, W. The German Satellite Mission TerraSAR-X. In Proceedings of the 2008 IEEE Radar Conference, Rome, Italy, 26–30 May 2008; pp. 306–310.
2. Zink, M.; Bartusch, M.; Miller, D. TanDEM-X Mission Status. In Proceedings of the 30th International Geoscience And Remote Sensing Symposium, Vancouver, BC, Canada, 24–29 July 2011.
3. Kraus, T.; Bräutigam, B.; Mittermayer, J.; Wollstadt, S.; Grigorov, C. TerraSAR-X Staring Spotlight Mode Optimization and Global Performance Predictions. *IEEE J. Sel. Top. Appl. Earth Observ. Remote Sens.* **2016**, *9*, 1015–1027. [CrossRef]

4. Buckreuss, S.; Schättler, B.; Fritz, T.; Steinbrecher, U.; Böer, J.; Bachmann, M.; Mittermayer, J.; Maurer, E.; Kahle, R.; Mrowka, F.; et al. Ten Years of TerraSAR-X Operations. *Remote Sens.* **2018**, under review.
5. Schwerdt, M.; Bräutigam, B.; Bachmann, M.; Döring, B.; Schrank, D.; Gonzalez, J.H. Final TerraSAR-X Calibration Results Based on Novel Efficient Calibration Methods. *IEEE Trans. Geosci. Remote Sens.* **2010**, *48*, 677–689. [CrossRef]
6. Schwerdt, M.; Gonzalez, J.H.; Bachmann, M.; Schrank, D.; Döring, B.; Ramon, N.T.; Antony, J.W. In-Orbit Calibration of the TanDEM-X System. In Proceedings of the 2011 IEEE International Geoscience and Remote Sensing Symposium, Vancouver, BC, Canada, 24–29 July 2011; pp. 2420–2423.
7. Schwerdt, M.; Schrank, D.; Bachmann, M.; Schulz, C.; Döring, B.; Gonzalez, J.H. TerraSAR-X Re-Calibration and Dual Receive Antenna Campaigns performed in 2009. In Proceedings of the 8th European Conference on Synthetic Aperture Radar, Aachen, Germany, 7–10 June 2010.
8. Grafmüller, B.; Herschlein, A.; Fischer, C. The TerraSAR-X Antenna System. In Proceedings of the 2005 IEEE International Radar Confrerence, Arlington, VA, USA, 9–12 May 2005; pp. 222–225.
9. Stangl, M.; Werninghaus, R.; Schweizer, B.; Fischer, C.; Brandfass, M.; Mittermayer, J.; Breit, H. TerraSAR-X Technologies and First Results. *IEE Radar Sonar Navig.* **2006**, *153*, 86–95. [CrossRef]
10. Schwerdt, M.; Hounam, D.; Alvarez-Pérez, J.L.; Molkenthin, T. The Calibration Concept of TerraSAR-X, a Multiple Mode High Resolution SAR. *Can. J. Remote Sens.* **2005**, *31*, 30–36. [CrossRef]
11. Döring, B.; Schwerdt, M.; Bauer, R. TerraSAR-X Calibration Ground Equipment. In Proceedings of the European Radar Conference, Munich, Germany, 10–12 October 2007.
12. Bräutigam, B.; Rizzoli, P.; González, C.; Schulze, D.; Schwerdt, M. SAR Performance of TerraSAR-X Mission with Two Satellites. In Proceedings of the 8th European Conference on Synthetic Aperture Radar, Aachen, Germany, 7–10 June 2010.
13. Bräutigam, B.; Schwerdt, M.; Bachmann, M. An Efficient Method for Performance Monitoring of Active Phased Array Antennas. *IEEE Trans. Geosci. Remote Sens.* **2009**, *47*, 1236–1243. [CrossRef]
14. Bachmann, M.; Schwerdt, M.; Brautigam, B. TerraSAR-X Antenna Calibration and Monitoring Based on a Precise Antenna Model. *IEEE Trans. Geosci. Remote Sens.* **2010**, *48*, 690–701. [CrossRef]
15. Tous-Ramon, N.; Schrank, D.; Bachmann, M.; Alfonzo, G.C.; Polimeni, D.; Böer, J.; Schwerdt, M. Long Term System Monitoring Status of the TerraSAR-X and the TanDEM-X Satellites. In Proceedings of the 9th European Conference on Synthetic Aperture Radar, Nuremberg, Germany, 23–26 April 2012; pp. 1–4.
16. Hounam, D.; Schwerdt, M.; Zink, M. Active Antenna Module Characterisation by Pseudo-Noise Gating. In Proceedings of the 25th ESA Antenna Workshop on Satellite Antenna Technology, Noordwijk, The Netherlands, 18–20 September 2002.
17. Bachmann, M.; Schwerdt, M.; Bräutigam, B. Accurate Antenna Pattern Modeling for Phased Array Antennas in SAR Applications—Demonstration on TerraSAR-X. *Int. J. Antennas Propag.* **2009**, *2009*, 492505. [CrossRef]
18. Rizzoli, P.; Bräutigam, B.; Zink, M. TanDEM-X Large-Scale Study of Tropical Rainforest for Spaceborne SAR Calibration in X-Band. In Proceedings of the 10th European Conference on Synthetic Aperture Radar, Berlin, Germany, 3–5 June 2014; pp. 1–4.
19. Danklmayer, A.; Döring, B.; Schwerdt, M.; Chandra, M. Assessment of Atmospheric Propoagation Effects in SAR Images. *IEEE Trans. Geosci. Remote Sens.* **2009**, *47*, 3507–3518. [CrossRef]